International Scientific Conference 20 UNITECH 26

INTERNATIONAL SCIENTIFIC CONFERENCE
19-21 November 2026
GABROVO

GLASS TRANSITION AND ATOMIC STRUCTURE OF RAPIDLY QUENCHED LIQUID METALLIC ALLOYS: A MOLECULAR DYNAMICS STUDY

Unal Domekeli[1,*], Figen Fuştanlı[2]

[1]*Dept. of Physics, Trakya University, 22030, Edirne – Türkiye*
[2]*Dept. of Physics, Institute of Science, Trakya University, 22030, Edirne – Türkiye*

……
**Corresponding author: unaldomekeli@trakya.edu.tr*

Abstract

Rapid cooling processes can facilitate the formation of a glassy structure by suppressing crystal nucleation and growth in metallic liquids. Despite their superior properties, such as high strength, the limited plastic deformation capability of metallic glasses poses a significant disadvantage. Therefore, understanding glass formation mechanisms and atomic structure is crucial for enhancing the properties of these materials. In this study, the glass formation behavior of the liquid $Zr_{54}Cu_{46}$ metallic alloy during rapid cooling was investigated using classical molecular dynamics (MD) simulations. The Embedded Atom Method (EAM) was employed to describe interatomic interactions, and simulations were conducted at three different cooling rates to examine the effect of the cooling rate. The glass transition temperature was determined based on the temperature-dependent changes in the total energy and volume of the system. Changes in local atomic structures and structural order during cooling were investigated using pair distribution function (PDF) analysis. The results show that the cooling rate significantly affects the glass transition temperature. It was observed that as the cooling rate increases, the glass transition temperature shifts to higher values, while at lower cooling rates it occurs at lower temperatures.

Keywords: Metallic glasses, glass transition temperature, MD simulation.

INTRODUCTION

In recent years, metallic glass materials lacking a long-range atomic order have become a significant area of research due to their superior mechanical properties, such as high strength and a wide range of elastic deformation [1,2]. The fact that their yield strengths are generally 2–3 times higher than those of traditional crystalline alloys and that they can reach an elastic strain limit of approximately 2 per cent makes these materials particularly important for engineering applications requiring high performance [3,4]. Metallic glasses are produced by solidifying a molten metallic liquid at sufficiently high cooling rates; as a result of the suppression of crystal nucleation and growth processes during rapid cooling, the disordered atomic structure characteristic of the liquid phase is preserved [5,6]. For this reason, metallic glasses are often defined as frozen liquids. However, the absence of long-range order in their atomic structures and their high structural disorder make it difficult to understand the glass-forming mechanism and local atomic structures [7]. The difficulty of experimentally tracking atomic movements and structural changes over time during rapid cooling makes MD simulations a vital tool for investigations at the atomic scale. Zr-based metallic glasses are of particular importance due to properties such as high strength and good ductility [8–10]. In particular, Zr–Cu alloys have been extensively investigated through experimental studies and MD simulations due to their high glass-forming ability and

This is an open access article licensed under Creative Commons Attribution 4.0 International
Print ISSN: 1313-230X, Online ISSN: 3033-1404

characteristic local atomic structures [11–15]. These studies have made significant contributions to our understanding of the effects of temperature, pressure, composition, annealing and cooling conditions on the atomic structure and glass-forming behavior of Zr–Cu systems. In particular, it has been reported that a distinct icosahedral short-range order is present in the $Zr_{54}Cu_{46}$ alloy and that the cooling rate affects the distances between free volumes and nearest-neighbor atoms [11]. However, it is evident that there is a limited number of studies examining how the glass transition temperature, as well as local atomic structures and dominant atomic clusters, change jointly and systematically at different cooling rates. In particular, atomic rearrangements, the formation of local atomic clusters and their relationship with the glass transition temperature are important for understanding the glass-forming mechanism.

In this study, the glass-forming behavior of the $Zr_{54}Cu_{46}$ alloy during rapid cooling was investigated at three different cooling rates using classical MD simulations. The glass transition temperature was determined from the temperature-dependent changes in total energy and volume; atomic and local structural changes were evaluated using pair distribution functions and local atomic structure analyses. Furthermore, the formation and temperature- and time-dependent evolution of dominant atomic configurations and clusters were investigated.

EXPOSITION

MD simulations were performed using the DLPOLY software, which enables high-performance parallel computing [16]. In MD simulations, the EAM set developed by Sheng [17] was used to characterize interatomic interactions. Periodic boundary conditions were applied in all simulations, and a supercell containing 8192 atoms was used to eliminate surface effects. The initial structure was constructed based on the B2 crystal structure with a $Cu_{50}Zr_{50}$ composition, representing the stable crystalline phase. To achieve the target $Zr_{54}Cu_{46}$ composition, 328 Cu atoms were randomly selected and replaced with an equal number of Zr atoms, thereby introducing controlled chemical disorder. This initial structure was used to investigate the amorphization and phase transformation behaviors of the alloy. The simulations were conducted using the NPT MD method, representing constant temperature and pressure conditions. Numerical integration was performed using the Leapfrog-Verlet algorithm with a time step of 1 fs; temperature and pressure were controlled via the Nosé-Hoover thermostat and the Berendsen barostat, respectively [18,19]. NPT-MD simulations were carried out over a temperature range of 0–2200 K in increments of 50 K. At each temperature, 100,000 MD steps were executed; the first 50,000 steps served for equilibration, while the subsequent 50,000 steps constituted the production phase used for calculating physical properties. After stabilizing the system in the liquid phase, controlled cooling was applied from 2200 K down to 0 K in 50 K reduced. Three different cooling rates 0.05 K/ps, 0.5 K/ps, and 5 K/ps were used to investigate the effect of cooling rate on structural transformation and glass transition behavior.

Figure 1 presents the temperature dependence of the total energy and volume of the $Zr_{54}Cu_{46}$ alloy during heating and cooling processes. As shown in Figure 1(a), the total energy exhibits an approximately linear increase with rising temperature up to the melting point during the heating process. This behavior arises from the atoms in the crystalline phase possessing higher vibrational energies as the temperature increases. A sudden and distinct jump in total energy occurs at approximately meting temperature (T_m) (T_m=1550 K). This discontinuity is a characteristic indicator of a first-order phase transition, representing the system's transformation from the crystalline phase to the liquid phase. At this point, the energy supplied to the system is

consumed to break down the crystalline structure and form the liquid phase, rather than to increase the temperature. Above the melting temperature, the system transitions entirely into the liquid phase, and the total energy resumes a linear increase with temperature. The fact that the energy curves for the heating and cooling processes overlap in the liquid phase region indicates that the cooling rate applied in the simulation is sufficient to prevent any crystal nucleation or recrystallization at high temperatures. Furthermore, this demonstrates that the system loses its structural memory after melting, exhibits stable liquid-phase behavior, and that the atoms possess high mobility. Upon examination of the cooling curve, unlike the melting transition observed during heating, the total energy changes continuously with temperature, and no sudden drop or discontinuity in energy occurs throughout the cooling process. This indicates that crystallization does not take place in the system and that the structure cools while retaining its amorphous character. However, a distinct change in the slope of the total energy-temperature curve occurs at approximately 750 K. This change in slope indicates that atomic mobility decreases significantly and the system begins to transition from the supercooled liquid state to the glassy state. Consequently, this temperature range can be associated with the glass transition temperature (T_g). As is well known, the glass transition is not a thermodynamic phase transition in the classical sense; the abrupt changes in volume and energy observed in first-order phase transitions do not occur during the glass transition. Figure 1(b) shows the variation of volume as a function of temperature during heating and cooling cycles. Similar to the energy curve, the volume increases linearly with temperature during the heating process up to the vicinity of the melting point. At the melting point, a sudden jump and a discontinuity occur in the volume. At temperatures above the melting point, the volume curve continues to increase linearly with temperature. Again, the volume curves for the heating and cooling processes overlap in the liquid region. During cooling, the slope of the volume-temperature curve changes markedly around 750 K, just as it does for the energy curve. This behavior is a significant indicator that a glassy structure is beginning to form in the system. The glasses transition temperature is defined as the intersection point of extrapolations of linear regions representing the liquid and glassy phases on the volume-temperature curve.

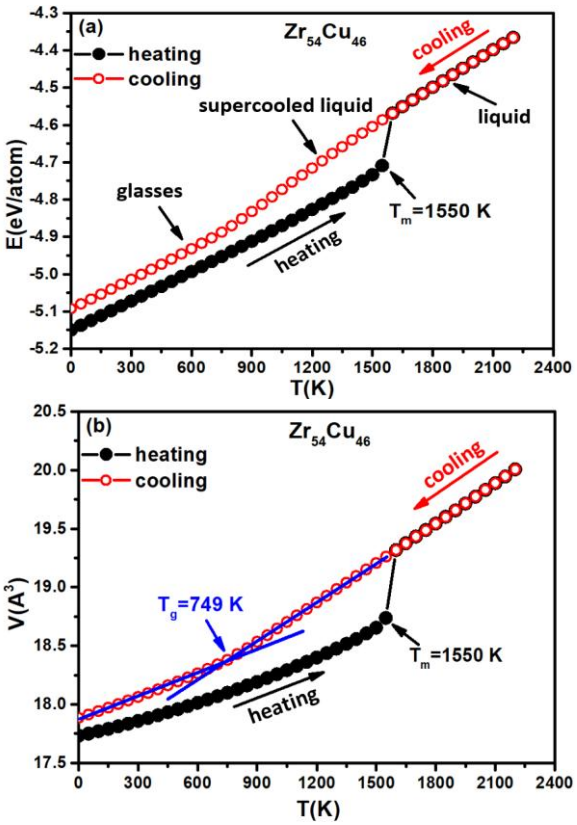


Fig. 1. *Variation of (a) the total energy and (b) the volume of the $Zr_{54}Cu_{46}$ alloy as a function of temperature at a heating and cooling rate of 0.5 K/ps*

Figure 2 shows the temperature-dependent change in volume at three different cooling rates: 0.05, 0.5, and 5.0 K/ps. As a result of linear fit, the glass transition temperatures for cooling rates of 0.05 K/ps, 0.5 K/ps, and 5.0 K/ps were determined to be 716 K, 749 K, and 769 K, respectively. As the cooling rate increases, the glass transition temperature rises. The main reason for this is that at high cooling rates, atoms do not have enough relaxation time to reach their

equilibrium configurations. This leads to the system being kinetically trapped in higher-energy and disordered structures.

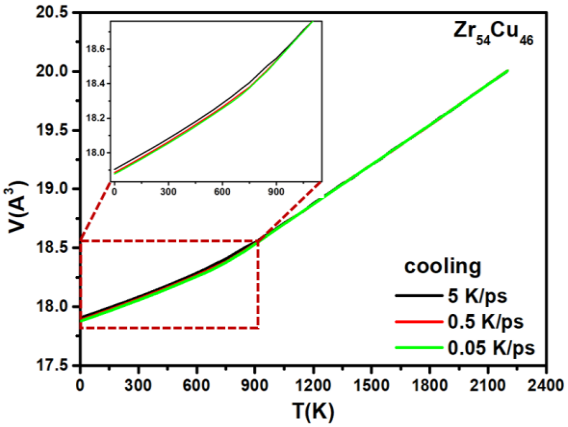


Fig. 2. *Temperature-dependent volume change of $Zr_{54}Cu_{46}$ alloy at different cooling rates.*

The pair distribution function (PDF) is a widely used method for quantitatively characterizing the atomic structure and short-range order of liquid and amorphous systems. This method quantitatively describes the spatial distribution of atomic order within the system and provides important information about short-range order. The PDF, g(r), can be calculated using the following expression [11]:

$$g(r) = \frac{V}{N^2}\langle\sum_{i=1}^{n}\frac{n(r)}{4\pi r^2\Delta r}\rangle, \quad (1)$$

here, N represents the number of atoms in the simulation cell; V represents the volume of the same cell; and $n(r)$ represents the number of particles in the spherical shell between r and $r + \Delta r$. For the binary alloy system in this work, the partial PDF between different atomic types was calculated using the following equation [11]:

$$g_{\alpha\beta}(r) = \frac{V}{N_\alpha N_\beta}\langle\sum_{i=1}^{N_\alpha}\frac{n_{i\beta}(r)}{4\pi r^2\Delta r}\rangle, \quad (2)$$

where α and β represent atomic types. In Figure 3, the total PDF obtained at 950 K from the MD simulation with a cooling rate of 0.5 K/ps is compared with the experimental result obtained at 926 K by synchrotron X-ray scattering by [13]. The simulation results show a high degree of agreement with the experimental data. In particular, the agreement of the positions and amplitudes of the peaks of the first, second, and third coordination shells in the g(r) function with the experimental results shows that the atomistic model used successfully represents the local and mid-range atomic order. This agreement reveals that the EAM potentials used in the simulations can reliably describe interatomic interactions and metallic bonding characteristics.

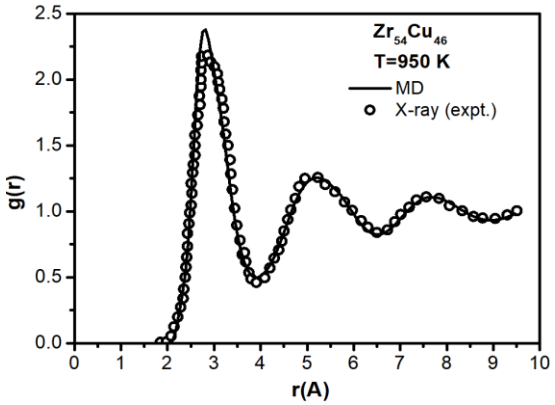
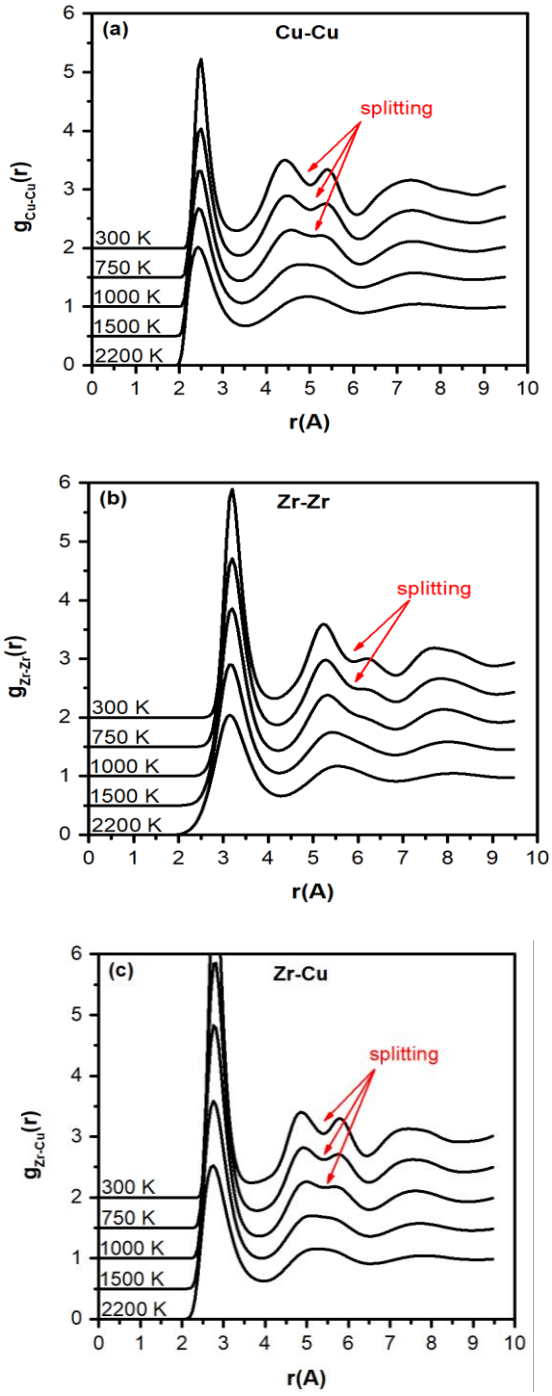


Fig. 3. *Comparison of total PDFs obtained from MD simulation and synchrotron X-ray scattering at a cooling rate of 0.5 K/ps.*

The structural evolution of the $Zr_{54}Cu_{46}$ alloy during the cooling process at a cooling rate of 0.5 K/ps was investigated using the partial and total pair distribution functions (PDFs) given in Figure 4(a-d). The peak splitting observed in the second coordination shell of the partial PDFs indicates the development of short and medium-range atomic order in the system and the beginning of the formation of local atomic clusters characteristic of the amorphous structure. However, it was determined that the splitting in the second peak did not occur at the same temperature for different atom pairs. This structural change became apparent at approximately 1000 K in Cu-Cu and Zr-Cu atom pairs, while it was observed at approximately 750 K in Zr-Zr atom pairs. This result shows that different atomic species contribute to the glass transition process at different temperature ranges and that the local atomic order develops differently depending on the chemical species. The total PDF results also reveal the structural transformation the system undergoes from liquid to amorphous with increasing temperature. The total PDF, exhibiting broad and irregular peak profiles

at high temperatures (2200 K), shows more pronounced peaks and strengthened interatomic correlations as the temperature decreases. At 750 K and 300 K, a splitting was observed in the second peak of the total PDF, consistent with the behavior observed in partial PDFs. However, the less pronounced splitting in the total PDF compared to partial PDFs is due to the overlapping of contributions from different pairs of atoms.



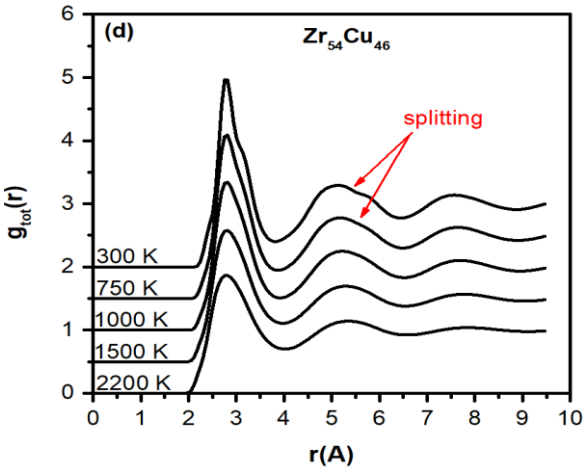


Fig. 4. *PDFs of $Zr_{54}Cu_{46}$ alloy: (a) Cu-Cu, (b) Zr-Zr, (c) Zr-Cu partial PDFs, and (d) total PDF*

Table 1: *Some physical quantities for Zr-Cu alloys.*

ZrCu (B2)		
E_c (eV)	*a* (Å)	Ω (Å^3)
5.06 (MD)	3.26 (MD)	17.36 (MD)
5.03[a] (Ab initio)	3.25[a] (Ab initio)	17.85[a] (Ab initio)
5.03[a] (other)		17.64[a] (other)
$Zr_{54}Cu_{46}$		
T_g (K)	T_m (K)	
749 (MD)	1550 (MD)	
696[a] (expt.)	1200[a] (expt.)	
R(Cu-Cu) (Å)	R(Zr-Cu) (Å)	R(Zr-Zr) (Å)
2.67 (MD)	2.78 (MD)	3.22 (MD)
2.53[a] (expt.)	2.75[a] (expt.)	3.15[a] (expt.)
2.50[a] (other)	2.76[a] (other)	3.19[a] (other)

[a]Ref. [11]

Comparison of the MD results in Table 1 with literature data shows that MD simulations performed using EAM potential can successfully characterize the structural and thermodynamic properties of Zr–Cu systems in both crystalline and amorphous structures. The lattice parameter (*a*), cohesive energy (E_c), and volume per atom (Ω) obtained for the crystalline $Zr_{50}Cu_{50}$ system were found to be consistent with ab initio and MD calculations in the literature. In the amorphous $Zr_{54}Cu_{46}$ alloy, the calculated glass transition temperature was approximately 7% higher than the experimental value, while the nearest neighbor atom distances of Cu–Cu, Zr–Cu, and Zr–Zr showed good agreement with the experimental data. These results demonstrate that the EAM potential can represent both equilibrium and bonding properties, as well as the short-range atomic order in the amorphous

structure, with sufficient accuracy, and offers a reliable approach for investigating Zr–Cu systems at the atomistic scale.

CONCLUSION

In this study, the thermodynamic and structural properties and glass-forming behavior of the metallic alloy $Zr_{54}Cu_{46}$ were investigated using MD simulations performed with EAM potential. The melting and glass transition processes of the system were characterized by analyzing the temperature-dependent changes of energy, volume, and pair distribution functions. The melting temperature of the alloy was determined to be approximately 1550 K, and it was observed that the glass transition temperature increased with increasing cooling rate. The cleavage observed at the second peak of the pair distribution functions at low temperatures revealed the formation of a short-range atomic order characteristic of the amorphous structure. The obtained results show that the EAM potential can successfully represent the structural and thermodynamic behavior of the $Zr_{54}Cu_{46}$ alloy and offers a suitable approach for the investigation of metallic glass formation at the atomic scale.

ACKNOWLEDGMENTS: *We would like to thank Trakya University Rectorate for giving permission and contributing to present this study as a paper.*

REFERENCE

[1] M. Chen, A brief overview of bulk metallic glasses, NPG Asia Mater. 3 (2011) 82–90.
[2] C. Suryanarayana, A. Inoue, Iron-based bulk metallic glasses, Int. Mater. Rev. 58 (2013) 131–166.
[3] W. L. Johnson, Bulk Glass-Forming Metallic Alloys: Science and Technology, MRS Bull. 24 (1999) 42–56.
[4] J. F. Löffler, Bulk metallic glasses, Intermetallics 11 (2003) 529–540.
[5] H. W. Sheng, E. Ma, M.J. Kramer, Relating Dynamic Properties to Atomic Structure in Metallic Glasses, JOM 64 (2012) 856–881.
[6] B. Karasu, A. O. Yanar, O. Erdoğan, S. Kartal, G. Ak, S.E. Pirangil, Metallic Glasses, Şişe Cam Tech. Bull. 45 (2017) 5.
[7] A. L. Greer, E. Ma, Bulk Metallic Glasses: At the Cutting Edge of Metals Research, MRS Bull. 32 (2007) 611–619.
[8] A. Inoue, W. Zhang, T. Zhang, K. Kurosaka, High-strength Cu-based bulk glassy alloys in Cu–Zr–Ti and Cu–Hf–Ti ternary systems, Acta Mater. 49 (2001) 2645–2652.
[9] A. Inoue, W. Zhang, T. Tsurui, A.R. Yavari, A.L. Greer, Unusual room-temperature compressive plasticity in nanocrystal-toughened bulk copper-zirconium glass, Philos. Mag. Lett. 85 (2005) 221–237.
[10] D. V. Louzguine, H. Kato, A. Inoue, High-strength Cu-based crystal-glassy composite with enhanced ductility, Appl. Phys. Lett. 84 (2004) 1088–1089.
[11] G. Duan, D. Xu, Q. Zhang, G. Zhang, T. Cagin, W.L. Johnson, W.A. Goddard, Molecular dynamics study of the binary $Cu_{46}Zr_{54}$ metallic glass motivated by experiments: Glass formation and atomic-level structure, Phys. Rev. B 71 (2005) 224208.
[12] M. I. Mendelev, Y. Sun, F. Zhang, C.Z. Wang, K.M. Ho, Development of a semi-empirical potential suitable for molecular dynamics simulation of vitrification in Cu-Zr alloys, J. Chem. Phys. 151 (2019).
[13] R. Dai, J.C. Neuefeind, D.G. Quirinale, K.F. Kelton, X-ray and neutron scattering measurements of ordering in a $Cu_{46}Zr_{54}$ liquid, J. Chem. Phys. 152 (2020).
[14] P. Dziegielewski, G. Evangelakis, J. Antonowicz, Short-to-medium range atomic order of Zr-Cu metallic glasses under compression, Comput. Mater. Sci. 208 (2022) 111345.
[15] J. Bi, X. Liu, H. Zhao, R. Li, T. Zhang, Rapid identification of highly glass-forming alloys in Cu–Zr binary system by laser glazing, Surf. Coatings Technol. 478 (2024) 130421.
[16] W. Smith, T.R. Forester, DL_POLY_2.0: A general-purpose parallel molecular dynamics simulation package, J. Mol. Graph. 14 (1996) 136–141.
[17] H. Sheng, EAM potentials, (2026). https://sites.google.com/site/eampotentials/table/cu-zr.
[18] S. Nose, A unified formulation of the constant temperature molecular dynamics methods, J. Chem. Phys. 81 (1984) 511.
[19] H.J.C. Berendsen, J.P.M. Postma, W.F. van Gunsteren, A. DiNola, J.R. Haak, Molecular dynamics with coupling to an external bath, J. Chem. Phys. 81 (1984) 3684–3690.